



Title	An allometric smoothing function to describe the relation between otolith and somatic growth over the lifespan of walleye pollock (<i>Theragra chalcogramma</i>)
Author(s)	Katakura, Seiji; Ikeda, Hisatoshi; Nishimura, Akira; Nishiyama, Tsuneo; Sakurai, Yasunori
Citation	Fishery Bulletin, 105(4), 447-456
Issue Date	2007
Doc URL	http://hdl.handle.net/2115/35249
Type	article
File Information	sakurai-74.pdf



[Instructions for use](#)

Abstract—We propose a new equation to describe the relation between otolith length (OL) and somatic length (fork length [FL]) of fish for the entire lifespan of the fish. The equation was developed by applying a mathematical smoothing method based on an allometric equation with a constant term for walleye pollock (*Theragra chalcogramma*)—a species that shows an extended longevity (>20 years). The most appropriate equation for defining the relation between OL and FL was a four-phase allometric smoothing function with three inflection points. The inflection points correspond to the timing of settlement of walleye pollock, changes in sexual maturity, and direction of otolith growth. Allometric smoothing functions describing the relation between short otolith radius and FL, long otolith radius and FL, and FL and body weight were also developed. The proposed allometric smoothing functions cover the entire lifespan of walleye pollock. We term these equations “allometric smoothing functions for otolith and somatic growth over the lifespan of walleye pollock.”

An allometric smoothing function to describe the relation between otolith and somatic growth over the lifespan of walleye pollock (*Theragra chalcogramma*)

Seiji Katakura (contact author)¹

Hisatoshi Ikeda²

Akira Nishimura¹

Tsuneo Nishiyama³

Yasunori Sakurai²

Email address for S. Katakura: seijika@fra.affrc.go.jp

¹ Hokkaido National Fisheries Research Institute
116, Katsurakoi, Kushiro
Hokkaido 085-0802, Japan

² Graduate School of Fisheries Sciences
Hokkaido University, 3-1-1, Minato-cho, Hakodate
Hokkaido 041-8611, Japan

³ Department of Marine Sciences and Technology
Hokkaido Tokai University, 5-1-1-1, Minamisawa, Minami-ku
Sapporo, Hokkaido 005-8601, Japan

The power function $y = ax^b$, used as an allometric equation (Huxley, 1924), is a useful tool for growth analysis of organisms. Equations that describe the relation between fish otolith length (OL: distance between the tip of rostrum and tip of postrostrum) and somatic length (e.g., fork length; FL: distance between the tip of head and fork of tail fin) have been widely used in fishery biology and ecological studies to estimate somatic length at younger ages with back-calculation methods. These methods are based on linear equations, log-transformed allometric equations, and quadratic equations (reviewed by Francis, 1990). However, these previous equations do not adequately reflect the complex changes in growth over the lifetime of a fish, especially for long-lived species.

Walleye pollock (*Theragra chalcogramma* (Pallas)) is the most abundant fish in the Bering Sea, constitutes the majority of the commercial catches from this area (Wespestad, 1993), and is a long-lived species. The oldest recorded age for this species is 28 years (McFarlane and Beamish, 1990). Juvenile walleye pollock serve

as a substantial prey source for older walleye pollock, other fish species, marine mammals, and sea birds. Thus, the year-class strength and population dynamics of walleye pollock have a significant influence on the entire ecosystem (Springer, 1992; Hunt et al., 2002). Estimations of somatic length and growth analyses at particular ages or life stages are imperative for fishery biology and ecological studies of walleye pollock.

In studies of the growth of walleye pollock, the equation that describes the relation between OL and somatic length (i.e., fork length) (referred to as the “OL-FL equation” in this article) is required in order to reconstruct the size of walleye pollock from otoliths collected from the stomachs of predators. Frost and Lowry (1981) applied two linear equations, with an inflection point at 10 mm OL, corresponding to 220 mm FL, in a total size range of 60–570 mm FL. Nishimura and Yamada (1988) applied the log-transformed allometric equation of the three linear equations with log-transformed OL and total length (TL: distance between the tip of head and tip of tail fin; 4.6–

680 mm) to data for three stages: larval stage (4.6–14.0 mm TL), juvenile stage (11–96 mm TL), and young-adult stage (88–680 mm TL). Zeppelin et al. (2004) adapted a quadratic equation for a fish size range of 49–530 mm FL. These previous equations allowed researchers to characterize the growth patterns of walleye pollock by regression analysis (the least-squares method), but they have several shortcomings because somatic length is not estimated across the whole life span of the fish. First, the equations, each of which represents a different life stage, do not facilitate comprehension of the continuity of each life stage. The equations are fitted to each segment of the data separately by inflection points that are derived from empirical data or visually from the scatter plots. Second, the quadratic equation has limitation in the shape of its curve which does not show the inflection point. The complex growth patterns are not adequately reflected in the equation. Third, the least-squares method does not allow for the incorporation of increasing variance with increasing fish length. When the sample distribution is biased, the calculated equation is largely influenced by the range of fish lengths from the largest number of samples. Fourth, previous OL-FL equations were not considered objectively in the selection of an adequate equation. No attempt has been made to apply information criteria such as Akaike's information criterion (AIC: Akaike, 1974), which is an operational way of trading off the complexity of an estimated equation against how well the equation fits the data.

To overcome these problems, we developed a new OL-FL equation for the whole lifespan of walleye pollock using a proposed allometric smoothing function to describe the relation between OL and FL. We also derived three distinctive allometric smoothing functions to establish the relationships between the short otolith radius (SOR: from core to the tip of rostrum) and FL, between the long otolith radius (LOR: from core to the tip of postrostrum) and FL, and between the FL and body weight (BW: wet body weight).

Materials and methods

General equations

The general equations in this analysis are linear equations (Eqs. 1 and 2), an allometric equation (Eq. 3), and an allometric equation with a constant term (Eq. 4):

$$y = ax \quad (1)$$

$$y = ax + c \quad (2)$$

$$y = ax^b \quad (3)$$

$$y = ax^b + c \quad (4)$$

where x = the independent variable;
 y = the dependent variable; and
 a , b , and c = parameters.

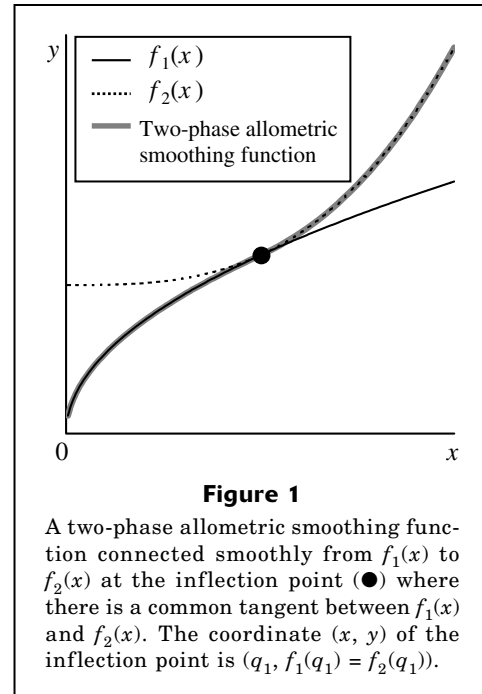


Figure 1

A two-phase allometric smoothing function connected smoothly from $f_1(x)$ to $f_2(x)$ at the inflection point (●) where there is a common tangent between $f_1(x)$ and $f_2(x)$. The coordinate (x, y) of the inflection point is $(q_1, f_1(q_1) = f_2(q_1))$.

Allometric smoothing function

A new OL-FL equation was developed by using a mathematical smoothing method based on an allometric equation with a constant term. The assumption of the allometric smoothing function was to have a common tangent at the inflection point to reflect the variable allometric growth smoothly. A composite of two or more allometric smoothing functions was defined as follows:

$$\delta_i(x) = \begin{cases} 1 & (q_{i-1} \leq x \leq q_i) \\ 0 & (x < q_{i-1}, q_i < x) \end{cases} \quad (5)$$

$$f_i(x) = \delta_i(x)(a_i x^{b_i} + c_i),$$

where $\delta_i(x)$ = switch function;

q_i = a value of x on the inflection point, here $q_0 = 0$;

$f_i(x)$ = a number i of function; and

a_i , b_i , and c_i = parameters for the function of i .

$f_i(x)$ is validated between the inflection points $(q_{i-1} \leq x \leq q_i)$ which depend on the $\delta_i(x)$.

We assumed that for the smooth integration of $f_i(x)$ and $f_{i+1}(x)$ (the function on the next order of i), both functions must pass through the inflection point $(x, y) = (q_i, f_i(q_i) = f_{i+1}(q_i))$ and have a common tangent at this point (Fig. 1). To satisfy the above conditions, the following two equations must be equal.

$$f_i(q_i) = f_{i+1}(q_i) \quad (6)$$

Table 1

The size ranges (in terms of length and weight) of walleye pollock (*Theragra chalcogramma*) examined in the Bering Sea during 1983–2002 to describe the relation between x (the independent variable) and y (the dependent variable). OL = otolith length; FL = fork length; SOR = short otolith radius; LOR = long otolith radius; and BW = body weight.

The variables (x [left below] and y [right below])	Range of x		Range of y		Number of samples (n)
	Minimum	Maximum	Minimum	Maximum	
OL (mm) and FL (mm)	2.27×10^{-2}	25.98	4.56	803	2354
SOR (mm) and FL (mm)	9.22×10^{-3}	11.80	4.56	803	1752
LOR (mm) and FL (mm)	1.22×10^{-2}	14.50	4.56	803	1704
FL (mm) and BW (g)	35.88	803	0.24	3014	2891

$$f'_i(q_i) = f'_{i+1}(q_i). \quad (7)$$

When Equation 5 is substituted for Equations 6 and 7, the following equations are obtained:

$$a_i q_i^{b_i} + c_i = a_{i+1} q_i^{b_{i+1}} + c_{i+1} \quad (8)$$

$$a_i b_i q_i^{b_i-1} = a_{i+1} b_{i+1} q_i^{b_{i+1}-1}. \quad (9)$$

Solving Equations 8 and 9 simultaneously yields

$$a_{i+1} = \frac{a_i b_i}{b_{i+1}} q_i^{b_i-b_{i+1}} \quad (10)$$

$$c_{i+1} = a_i q_i^{b_i} \left(1 - \frac{b_i}{b_{i+1}} \right) + c_i. \quad (11)$$

The functions of $f_i(x)$ and $f_{i+1}(x)$ can be smoothly connected at the inflection point if Equations 10 and 11 are equal. The formula of the allometric smoothing function y is shown as follows:

$$y = \sum_{i=1}^n f_i(x) = \sum_{i=1}^n \delta_i(x) (a_i x^{b_i} + c_i). \quad (12)$$

Fitting the OL-FL equations

The allometric smoothing function (Eq. 12) is fitted by using the maximum likelihood method. In the fitting, the sample distribution around the dependent variable was assumed to have a normal distribution. The estimated standard deviation (SD) for the dependent variable was used to calculate the weighted likelihood. The fitting procedure is shown as follows (see Appendix Table):

$$\hat{FL} = f_i(OL_j) = a_i OL_j^{b_i} + c_i + \varepsilon_j \quad (q_{i-1} \leq OL_j \leq q_i), \quad (13)$$

where \hat{FL}_j = the calculated FL for individual j ;
 OL_j = the measured OL of individual j ; and
 ε_j = the error for individual j .

Equation 13 is validated between the inflection points ($q_{i-1} \leq OL_j \leq q_i$).

The distribution of ε_j is assumed to have a normal distribution N (mean, variance) = $N(0, \hat{\sigma}_{FL_j}^2)$:

$$\hat{\sigma}_{FL_j} = dOL_j^e + f, \quad (14)$$

where $\hat{\sigma}_{FL_j}$ = the estimated SD of the FL of individual j ; and
 d , e , and f = parameters.

The variable $\hat{\sigma}_{FL_j}$ is assumed to fit the general equations (Eqs. 3 or 4).

To fit \hat{FL}_j to the general equations (Eqs. 1–3), the following procedures are used. For Equation 1, the parameters in Equation 13 are fixed as $b_i = 1$ and $c_i = 0$; for Equation 2, the parameter is fixed as $b_i = 1$; and for Equation 3, the parameter is fixed as $c_i = 0$.

A likelihood of measured FL is calculated by the following equations:

$$L_j = \frac{1}{\sqrt{2\pi}\hat{\sigma}_{FL_j}} \exp \left\{ -\frac{(FL_j - \hat{FL}_j)^2}{2\hat{\sigma}_{FL_j}^2} \right\} \quad (15)$$

and

$$LL = \sum_{j=1}^n \ln L_j, \quad (16)$$

where L_j = likelihood (the probability density) of FL_j ;
 FL_j = the measured FL of individual j ; and
 LL = a log-likelihood.

LL is maximized by changing the parameters.

Determination of the OL-FL equations

The equation with the minimum AIC was selected:

$$AIC = -2MLL + 2p \quad (17)$$

where MLL = the maximum LL and
 p = the number of parameters.

In the composite of two or more functions, a_i and c_i of $i \geq 2$ are calculated by Equations 10 and 11. Therefore, these parameters are not included in the number of parameters needed to calculate the AIC (see Appendix Table).

The upper and lower 95% confidence intervals (CI_j) of \hat{FL}_j were determined as follows:

$$CI_j = \hat{FL}_j \pm 1.96\hat{\sigma}_{FL_j}. \quad (18)$$

The equations for describing the relation between SOR and FL, LOR and FL, and FL and BW were calculated in the same way.

Application of equations to walleye pollock

Walleye pollock were collected and used as a model for long-lived species. The relevant biological data were collected, processed, and compiled from various cruise data conducted by Japanese and U.S. agencies at a total of 97 sampling stations in the Bering Sea (95 stations) and Chukchi Sea (northeastward extension of the Bering Sea; 2 stations) during 1983–2002 (Fig. 2).

In the central Bering Sea (Aleutian Basin), adult walleye pollock vary in age from 5 to >20 years (McFarlane and Beamish, 1990; Traynor et al., 1990). Young fish (0 to 4) are distributed on the continental shelf and slope and then migrate into the basin area beginning at age 5 (Traynor et al., 1990). In the present study, the samples of walleye pollock in the Bering Sea are presumed to have been collected from the same population of fish. Samples of juvenile walleye pollock at two discrete positions in the Chukchi Sea were also treated as originating from the Bering Sea. Larvae were sampled with a MOCNESS net, and juveniles and adults were captured with mid-water or bottom trawl nets. We measured the somatic length and BW of each fish and removed its otoliths (sagittae). For walleye pollock larger than 15 mm in somatic length, we measured FL, and for those smaller than 15 mm (with undeveloped fin rays), we measured TL. Difference in FL and TL was negligible in fish <15 mm; therefore TL is referred to as FL in the present analysis.

Specimens examined in the present study ranged from 4.56 mm to 803 mm FL. The number of samples used in the analysis of OL-FL equations is given in Table 1, as well as the size range of otolith measures and fish sizes. The approximate length of newly hatched larvae is 4.6 mm FL (=TL), 0.02 mm OL, and 0.01 mm SOR and LOR.

The relation between OL and FL was fitted to the general equations (Eqs. 1–4) and the allometric smoothing function (Eq. 12). The equations for describing the relation between SOR and FL, LOR and FL, and FL and BW were calculated in the same way.

Otolith processing

For measurement of SOR and LOR, the left or right otolith was selected and processed as a frontal section

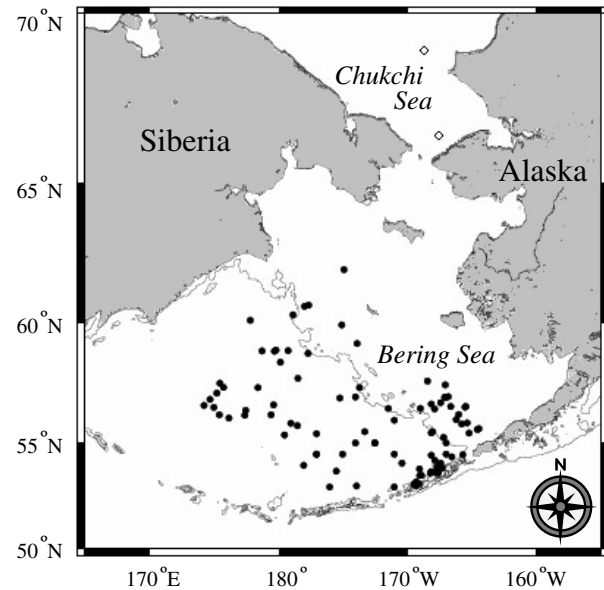


Figure 2

Map showing the sampling locations for walleye pollock (*Theragra chalcogramma*) in the present study. There were 97 total sampling stations: Bering Sea (●: 95 stations) and Chukchi Sea (○: 2 stations) in 1983–2002.

to reveal the perpendicular structure of the proximal surface, including the tips of rostrum and postrostrum, and core (Fig. 3A). The procedure for otolith processing followed that of Secor et al. (1992).

Larval and juvenile otoliths were embedded in epoxy resin adhesive (Epoxy bond quick 5; Konishi Co., Ltd., Osaka, Japan) on a glass slide, and OL was measured under a microscope (SMZ-U or Labophot-2A; Nikon Co., Tokyo, Japan) by using an image analysis system (ARGUS-10; Hamamatsu Photonics K. K. Co., Shizuoka, Japan). The otolith was then carefully polished with wet sandpaper (no. 1200) and lapping paper (12–0.3 μ) as preparation for making the frontal section (Fig. 3B).

For the frontal section of large otoliths of postjuvenile and adult fish, the otolith proximal surface was placed facing up, and OL was measured. Then, the otolith proximal surface was marked at three points: the tip of the rostrum, the tip of the postrostrum, and the core region on the central concave area. The otolith was embedded in epoxy resin (Epoxicure; Buehler Ltd., Lake Bluff, IL) on a hardened epoxy bed about 3 mm deep in a plastic mold. The hardened epoxy block containing the otolith was cut and trimmed by a micro cutter (MC-201; Maruto Instrument Co., Ltd., Tokyo, Japan) to a 3-mm-wide section that included the three marks. The trimmed sample was fixed on a slide glass with hot wax (Stick wax; Maruto Instrument Co., Ltd., Tokyo, Japan) and polished with wet sandpaper (no. 400–800) on a polishing machine (ML-101; Maruto Instrument Co., Ltd., Tokyo, Japan and SBT900; South Bay Technology Inc., San Clemente, CA). Polishing was continued until the core and tips of the rostrum and postrostrum appeared. The polishing was also made on the opposite side of the

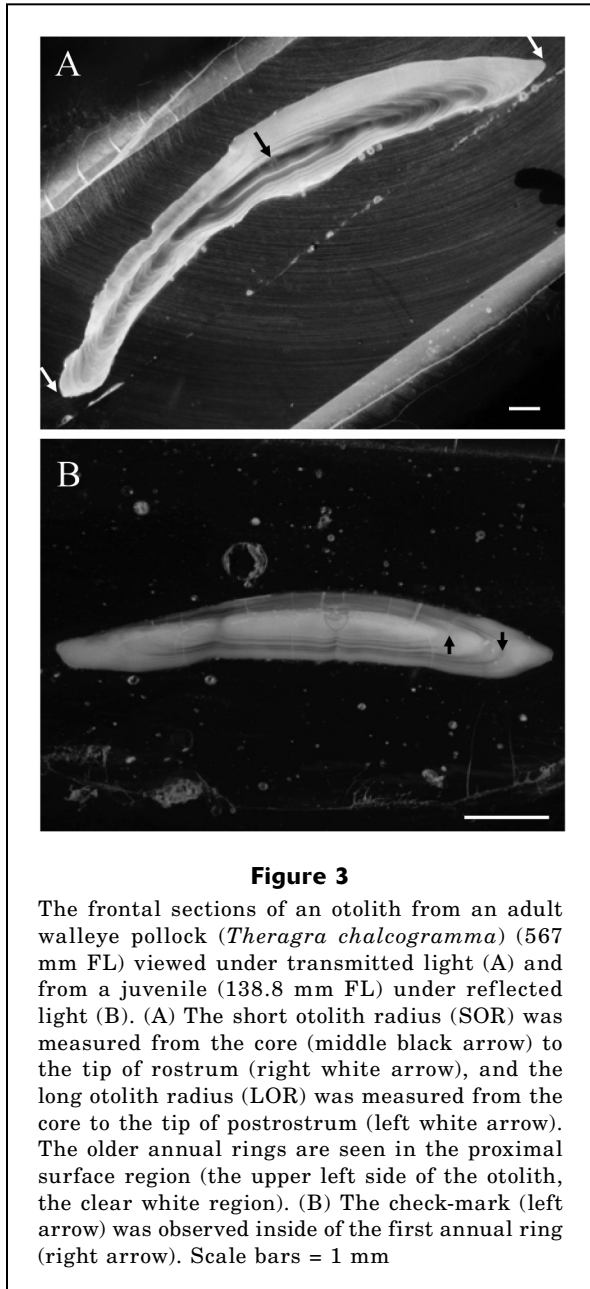


Figure 3

The frontal sections of an otolith from an adult walleye pollock (*Theragra chalcogramma*) (567 mm FL) viewed under transmitted light (A) and from a juvenile (138.8 mm FL) under reflected light (B). (A) The short otolith radius (SOR) was measured from the core (middle black arrow) to the tip of rostrum (right white arrow), and the long otolith radius (LOR) was measured from the core to the tip of postrostrum (left white arrow). The older annual rings are seen in the proximal surface region (the upper left side of the otolith, the clear white region). (B) The check-mark (left arrow) was observed inside of the first annual ring (right arrow). Scale bars = 1 mm

section. The section was finally polished by hand with wet sandpaper (no. 1200). The thickness of the polished frontal section (including the thickness of the wax) was 0.28 ± 0.07 mm (mean \pm SD, $n=50$). The OL in the frontal section shrank ($98.7 \pm 2.5\%$, $n=1775$) after the polishing; however the decrease was not analyzed in this study.

Results

Relation between otolith length (OL) and fork length (FL)

The most suitable equation to describe the OL (mm) and FL (mm) relationship chosen with the minimum AIC was

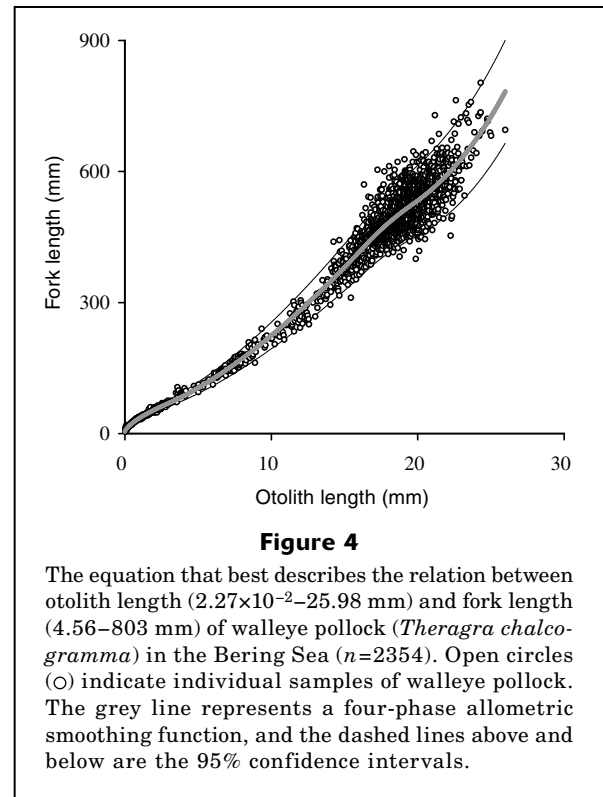


Figure 4

The equation that best describes the relation between otolith length (2.27×10^{-2} –25.98 mm) and fork length (4.56–803 mm) of walleye pollock (*Theragra chalcogramma*) in the Bering Sea ($n=2354$). Open circles (○) indicate individual samples of walleye pollock. The grey line represents a four-phase allometric smoothing function, and the dashed lines above and below are the 95% confidence intervals.

the four-phase allometric smoothing function (Fig. 4). The minimum AIC in the general equations was an allometric equation with a constant term (Eq. 4). In the AIC, all allometric smoothing functions produced lower estimates than all of the general equations. In the allometric smoothing functions, the AIC decreased with the number of allometric smoothing functions, which increased from two to four. However, the AIC in the five-allometric smoothing function was higher than that in the four-phase allometric smoothing function (Table 2). The relation between OL (mm) and $\hat{\sigma}_{FL}$ (mm) is given as follows:

$$FL = 31.55 OL^{0.67} + 4.05 \quad (0.00 < OL < 2.92) \quad (19.1)$$

$$FL = 5.64 OL^{1.51} + 40.11 \quad (2.92 \leq OL < 16.48) \quad (19.2)$$

$$FL = -26083.56 OL^{-1.49} + 831.85 \quad (16.48 \leq OL < 19.65) \quad (19.3)$$

$$FL = 1.28 \times 10^{-4} OL^{4.56} + 424.57 \quad (19.65 \leq OL) \quad (19.4)$$

$$\hat{\sigma}_{FL} = 0.41 OL^{1.52} + 1.80. \quad (20)$$

The coordinates (OL, FL) of the three inflection points were found at (2.92, 68.7), (16.48, 433.0), and (19.65, 525.0).

Relation between short otolith radius (SOR) and fork length (FL)

For the relation between SOR (mm) and FL (mm), we fitted the general equations (Eqs. 1–4) and the allometric

Table 2

Types of equations, range of otolith length (OL), inflection points, parameters, and Akaike's information criterion (AIC) for the equations used to describe the relation between OL (2.27×10^{-2} –25.98 mm) and fork length (FL: 4.56–803 mm) of walleye pollock (*Theragra chalcogramma*) in the Bering Sea ($n = 2354$). The minimum AIC was the four-phase allometric smoothing function. Estimated standard deviation of FL ($\hat{\sigma}_{FL} = d OL^e + f$).

Relational equation types	Range of OL		Inflection points		Parameter for equations			Parameter for $\hat{\sigma}_{FL}$			AIC
	Minimum	Maximum	<i>OL</i>	<i>FL</i>	<i>a</i>	<i>b</i>	<i>c</i>	<i>d</i>	<i>e</i>	<i>f</i>	
General equations											
$FL = a\ OL$	—	—	—	—	26.42	—	—	3.16	0.81	6.77	22,820
$FL = a\ OL + c$	—	—	—	—	25.94	—	7.02	5.66	0.68	1.27	22,573
$FL = a\ OL^b$	—	—	—	—	21.37	1.07	—	1.28	1.07	9.73	22,706
$FL = a\ OL^b + c$	—	—	—	—	15.18	1.18	15.14	0.74	1.31	4.61	22,016
Allometric smoothing functions											
$FL = a_1\ OL^{b_1} + c_1$	0.00	2.25	—	—	32.41	0.64	3.34	0.41	1.54	1.76	21,194
$FL = a_2\ OL^{b_2} + c_2$	2.25	—	2.25	57.7	8.33	1.37	32.40				
$FL = a_1\ OL^{b_1} + c_1$	0.00	2.87	—	—	31.59	0.67	4.02	0.40	1.53	1.80	21,089
$FL = a_2\ OL^{b_2} + c_2$	2.87	15.58	2.87	68.0	5.81	1.50	39.56				
$FL = a_3\ OL^{b_3} + c_3$	15.58	—	15.58	400.7	3853.78	0.11	−4748.09				
$FL = a_1\ OL^{b_1} + c_1$	0.00	2.92	—	—	31.55	0.67	4.05	0.41	1.52	1.80	21,066
$FL = a_2\ OL^{b_2} + c_2$	2.92	16.48	2.92	68.7	5.64	1.51	40.11				
$FL = a_3\ OL^{b_3} + c_3$	16.48	19.65	16.48	433.0	−26083.56	−1.49	831.85				
$FL = a_4\ OL^{b_4} + c_4$	19.65	—	19.65	525.0	1.28×10 ^{−4}	4.56	424.57				
$FL = a_1\ OL^{b_1} + c_1$	0.00	2.92	—	—	31.54	0.67	4.06	0.41	1.52	1.80	21,069
$FL = a_2\ OL^{b_2} + c_2$	2.92	16.53	2.92	68.7	5.64	1.51	40.12				
$FL = a_3\ OL^{b_3} + c_3$	16.53	19.97	16.53	434.8	−35709.22	−1.63	800.80				
$FL = a_4\ OL^{b_4} + c_4$	19.97	20.42	19.97	532.0	9.28×10 ^{−17}	13.49	499.52				
$FL = a_5\ OL^{b_5} + c_5$	20.42	—	20.42	543.3	2.40×10 ^{−3}	3.68	382.98				

smoothing function (Eq. 12). The minimum AIC was the four-phase allometric smoothing function. The relation between SOR (mm) and $\hat{\sigma}_{FL}$ (mm) was also shown as follows:

$$FL = 55.18 SOR^{0.61} + 2.51 \quad (0.00 < SOR < 1.00) \quad (21.1)$$

$$FL = 24.22 SOR^{1.39} + 33.47 \quad (1.00 \leq SOR < 7.55) \quad (21.2)$$

$$FL = -55349.12 SOR^{-2.78} + 639.86 \quad (7.55 \leq SOR < 8.96) \quad (21.3)$$

$$FL = 6.68 \times 10^{-4} SOR^{5.25} + 447.65 \quad (8.96 \leq SOR) \quad (21.4)$$

$$\hat{\sigma}_{FL} = 2.19 SOR^{1.37} + 1.91. \quad (22)$$

The coordinates (SOR, FL) of the three inflection points were found at (1.00, 57.8), (7.55, 437.3), and (8.96, 514.1).

Relation between long otolith radius (LOR) and fork length (FL)

In a similar way, the relationship between LOR (mm) and FL (mm) was derived, and the minimum AIC was a four-phase allometric smoothing function. The rela-

tion between LOR (mm) and $\hat{\sigma}_{FL}$ (mm) is also shown as follows:

$$FL = 48.98 LOR^{0.65} + 3.26 \quad (0.00 < LOR < 1.54) \quad (23.1)$$

$$FL = 14.84 LOR^{1.48} + 39.86 \quad (1.54 \leq LOR < 9.03) \quad (23.2)$$

$$FL = -16116.83 LOR^{-1.77} + 754.41 \quad (9.03 \leq LOR < 11.30) \quad (23.3)$$

$$FL = 1.34 \times 10^{-4} LOR^{5.44} + 464.28 \quad (11.30 \leq LOR) \quad (23.4)$$

$$\hat{\sigma}_{FL} = 1.77 LOR^{1.32} + 1.85. \quad (24)$$

The coordinates (LOR, FL) of the three inflection points were found at (1.54, 68.1), (9.03, 428.8), and (11.30, 535.6).

Relation between fork length (FL) and body weight (BW) (g)

The relation between FL (mm) and BW (g) was fitted to the general equations (Eqs. 3 and 4), the allometric

smoothing function (Eq. 12), and an allometric smoothing function without a constant term in the first function ($c_1=0$). The minimum AIC was the three-phase allometric smoothing function without c_1 . The relation between FL (mm) and $\hat{\sigma}_{BW}$ (g) is shown as follows:

$$BW = 2.01 \times 10^{-5} FL^{2.77} \quad (0.00 < FL < 70.0) \quad (25.1)$$

$$BW = 6.61 \times 10^{-6} FL^{3.02} + 0.21 \quad (70.0 \leq FL < 431.2) \quad (25.2)$$

$$BW = 4.17 \times 10^{-6} FL^{3.09} + 13.89 \quad (431.2 \leq FL) \quad (25.3)$$

$$\hat{\sigma}_{BW} = 1.06 \times 10^{-5} FL^{2.63} \quad (26)$$

The coordinates (FL, BW) of the two inflection points were seen at (70.0, 2.6) and (431.2, 586.2).

Discussion

The allometric smoothing function

The best equation to describe the relation between OL and FL in walleye pollock throughout the entire lifespan of the fish was depicted by a four-phase allometric smoothing function with three inflection points. In our preliminary analysis, a quadratic equation was applied for the OL and FL relationship, and the resulting AIC was 21,743. This value was smaller than that derived from general equations, but was higher than the value derived from any of our allometric smoothing functions (see Table 2). The general equations and the quadratic equation do not adequately reflect the variable otolith and somatic allometric growth during the whole lifespan of the species.

Equations relating OL to somatic length have been developed to represent complex growth curves. Bervian et al. (2006) used an allometric equation transformed from the logistic function for the OL-TL relationship in whitemouth croaker (*Micropogonias furnieri*). Imai et al. (2002) applied a Gompertz model to the relation between otolith height and standard length in cyprinid fish “Ukekuchi-ugui” (*Tribolodon nakamura*). However, these two models have limitations in both the shape of the curve and the number of inflection points. If the species in the model, such as walleye pollock in this study, has more than two inflection points in the derived curve, these models cannot represent the allometric growth patterns adequately. Our present allometric smoothing function has no such limitation in the number of inflection points or the shape of curve between inflection points and responds appropriately to the growth pattern of the fish.

Our allometric smoothing function has the ability to satisfy both the needs for mathematical continuity (see Fig. 1) and objectivity in the selection of an equation (see Table 2) while allowing for biological events. The allometric smoothing function was developed by using a mathematical smoothing method based on an

allometric equation with a constant term. Among the smoothing methods available, the moving average, autoregression, and spline curve proved to be useful for fitting scatter sample plots, a type of plot that cannot be properly fitted in a single function. Nevertheless, the moving average requires that the modeler be subjective in determining the number of data points used to calculate the average. In contrast, the autoregression allows a measure of objectivity in selecting the equation; however steady growth conditions are assumed with this method. Finally, the spline curve is based on a multidimensional function developed by mathematical procedure where biological events were not taken into consideration.

Until recently, back-calculation models for individual fish growth have been developed to estimate past fish length and growth, under the assumption that fish growth is proportional to otolith growth (Francis, 1990). However, many studies have recognized that fish growth and otolith growth are uncoupled. “Growth rate effect” and “age effect” are two of the most important factors affecting uncoupling. The growth rate effect occurs when otoliths from slow growing fish are larger than those of fast growing fish, when these fish are compared at the same somatic length (Reznick, 1989; Campana, 1990; Secor and Dean, 1992). Adapting Campana’s (1990) biological intercept method can reduce the error inherent in back-calculated somatic length from this growth-rate effect. Additionally, with the back-calculation model developed by Morita and Matsuishi (2001), the fact that age effect on otolith size increases continuously during nongrowth periods (Mugiya, 1990; Secor and Dean, 1992) can be taken into account. The inclusion of these growth and age effects of individual fish to our allometric smoothing function provides a more accurate analysis of growth at the individual level in the back-calculation model.

Application of the allometric smoothing function for walleye pollock

Our best equation to describe the relation between OL and FL was derived as a four-phase allometric smoothing function with three inflection points (Fig. 4). In Huxley’s (1924) allometric equation ($y=ax^b$), relative growth rate was expressed by the relative growth coefficient (allometric coefficient, b). Our allometric smoothing function is based on the allometric equation with an added constant term ($y=ax^b + c$). The superscript b in our equation is not an allometric coefficient; it indicates the relative growth between x and y on the slope of the curve between inflection points.

The explicit changes in the shape of the curves and the appearance of inflection points in our equation imply that ecological and physiological changes are associated with unique aspects of life history of walleye pollock. In the first function (Eq. 19.1), somatic growth is slower than otolith growth, whereas in the second function (Eq. 19.2), somatic growth is faster than otolith growth. Concerning these contrasting

outcomes, previous findings indicate that possible ecological changes may have occurred at a particular size range, as evidenced by otolith characters such as the check-mark. Nishimura (1993) reported that 32% of age-1 walleye pollock caught in the Bering Sea revealed check-marks inside the first annual ring of the otolith and he concluded that the check-mark would have been formed at 40–80 mm FL (mode: 70 mm) at an age of 4 months. This check-mark was frequently detected in our samples (Fig. 3B). Similarly, in Funka Bay, Japan, 58% of age-1 walleye pollock had check-marks inside the first annual ring (Katakura et al., 2003). The settlement of juvenile walleye pollock from pelagic to benthic habitat began from 70 mm TL and was completed when the fish reached >85 mm TL in Funka Bay (Nakatani and Maeda, 1987). Our calculated FL at the first inflection point was 68.7 mm, which is approximately the same size as that when settlement begins. The check-mark on the otoliths of walleye pollock appears to occur, irrespective of differences in geographic features of inhabited waters. Victor (1982) suggested that the check-mark occurs as a settlement mark and indicates the occurrence of physiological changes or biological processes associated with settlement. Thus, we conclude that the first inflection point at a particular size in our allometric growth curve shows the adaptive response of walleye pollock to physiological and environmental changes at the time of settlement.

The state of $b < 0$ but $a < 0$ in the third function (Eq. 19.3) also implies that somatic growth is slower than otolith growth. The allometric coefficient between OL and somatic length drastically changes in association with sexual maturity (Bervian et al., 2006). The Bogoslof area in the Aleutian Basin is known as one of the main spawning grounds of walleye pollock in winter. In this area, fish length at maturity was 360–570 mm FL (mean 464 mm) in males and 370–610 mm FL (482 mm) in females (Traynor et al., 1990). The second inflection point that appeared at 433.0 mm FL in our study is situated within the size range of maturing fish. We assume that the fish length around the second inflection point corresponds to the timing of an energy shift from somatic growth to gonad development, and to corresponding changes that occur in the shifts of the allometric growth curve.

Both the third inflection point at 525.0 mm FL and the fourth function (Eq. 19.4) indicate faster somatic growth than otolith growth. Otolith growth persists despite the cessation of body growth (Mugiya, 1990; Secor and Dean, 1992); therefore, the otolith is also assumed to grow throughout the lifetime of walleye pollock (McFarlane and Beamish, 1990). Older annual rings appear on the ventral proximal surface region, as evidenced in the transverse section (McFarlane and Beamish, 1990), similar to those seen in the proximal surface region of the frontal section (Fig. 3A). The shape of the large otolith is an arched curve connecting the tip of the rostrum, core, and tip of the postrostrum. Thus, the third inflection point is con-

sidered to be closely related to the slow growth phase of otoliths, accompanying the change in the direction of growth in otoliths from length (between the tips of rostrum and postrostrum) to width (proximal surface region increasing), and an increase in the slope of the curve.

The best equations that describe the relation of SOR to FL, and LOR to FL were also represented by the four-phase allometric smoothing function with three inflection points (Eqs. 21.1–21.4 and 23.1–23.4). The characteristics of the allometric otolith and somatic growth patterns are similar, as found in the OL and FL relation. These relationships can be useful for the analysis of growth of juvenile walleye pollock from the back-calculation of adult otoliths. The measurements of the SOR or LOR of fish at young ages allow one to convert these measurements to FL values. Similarly, our equations allow the conversion of FL from any otolith measurement (OL, SOR, and LOR) into BW.

The resultant coordinates of the two inflection points at FL of 70.0 mm and 431.2 mm derived from our FL and BW relationship (Eqs. 25.1–25.3) were very close to the first (68.7 mm FL) and second (433.0 mm FL) inflection points that emerged in the OL and FL relationship (Eqs. 19.1–19.4). Because settlement and sexual maturity are distinct biological events in the life history of this fish, the timing of these events will be clearly demonstrated in allometric growth.

The condition factor (CF) of fish is generally calculated by a formula ($CF = 10^3 \times BW / FL^3$). However, our results indicate that the relation between FL and BW is not constant over the lifetime of walleye pollock, and probably for other fish species. In our equations, b increased as fish grew in association with life stages from $b_1 = 2.77$ to $b_2 = 3.02$ and $b_3 = 3.09$, and this inflation has potential implications for studies of fish growth.

The present equations can be applied to the reconstruction of size composition of fish from the remnant otoliths found in the digestive organs of predators. We expect that these reliable equations, with transformation of otolith measurement data into FL or BW values, are useful not only for fish growth analysis, but also for food habit and energetic studies (e.g., food conversion efficiency studies) because these studies rely substantially on the back-calculation method.

The samples of walleye pollock used in this study provided a range of fish lengths from 4.56 mm FL (=TL in larvae) to 803 mm FL. Newly hatched walleye pollock measure about 4.6 mm TL (Nishimura and Yamada, 1988), and the oldest fish reported from the Bering Sea was 28 years old and measured 530 mm FL (McFarlane and Beamish, 1990). Thus, the present data set can be regarded as including almost the entire size range of walleye pollock over the whole life span. Because the proposed allometric smoothing functions can be extensively applicable to all life stages of walleye pollock, we term these equations “allometric smoothing functions for otolith and somatic growth over the lifespan of walleye pollock.”

Acknowledgments

We thank J. R. Bower, K. Morita, N. J. Williamson, and the anonymous referees for invaluable advice on the manuscript, T. Yanagimoto, K. Mito, T. Honkalehto, S. de Blois, N. Tanimata, R. Nanbu, and O. Sakai for assistance with the sampling and measurements of fish samples. We also thank the scientists of the following agencies for the offer of biological data and otolith samples: National Research Institute of Far Seas Fisheries, Fisheries Research Agency, Japan; Hokkaido National Fisheries Research Institute, Fisheries Research Agency, Japan; Graduate School of Fisheries Sciences, Hokkaido University, Japan; and Alaska Fisheries Science Center, National Marine Fisheries Service, National Oceanic and Atmospheric Administration, USA. We also thank the crews of the RV *Kaiyo Maru*, TS *Oshoro Maru*, RV *Miller Freeman*, and chartered fishing vessels.

Literature cited

- Akaike, H.
1974. A new look at statistical model identification. IEEE (Institute of Electrical and Electronics Engineers, Inc.) Transactions on Automatic Control 19:716–723.
- Bervian, G., N. F. Fontoura, and M. Haimovici.
2006. Statistical model of variable allometric growth: otolith growth in *Micropogonias furnieri* (Actinopterygii, Sciaenidae). J. Fish Biol. 68:196–208.
- Campana, S. E.
1990. How reliable are growth back-calculations based on otoliths? Can. J. Fish. Aquat. Sci. 47:2219–2227.
- Francis, R. I. C. C.
1990. Back-calculation of fish length: a critical review. J. Fish Biol. 36:883–902.
- Frost, K. J., and L. F. Lowry.
1981. Trophic importance of some marine gadids in northern Alaska and their body-otolith size relationships. Fish. Bull. 79:187–192.
- Hunt, G. L., P. Staben, G. Walters, E. Sinclair, R. D. Brodeur, J. M. Napp, and N. A. Bond.
2002. Climate change and control of the southeastern Bering Sea pelagic ecosystem. Deep-Sea Res. II 49:5821–5853.
- Huxley, J. S.
1924. Constant differential growth-ratios and their significance. Nature 14:895–896.
- Imai, C., H. Sakai, K. Katsura, W. Honto, Y. Hida, and T. Takazawa.
2002. Growth model for the endangered cyprinid fish *Tribolodon nakamura* based on otolith analyses. Fish. Sci. 68:843–848.
- Katakura, S., M. Ohta, M. Jin, and Y. Sakurai.
2003. Otolith-marking experiments of juvenile walleye pollock *Theragra chalcogramma* using oxytetracycline, alizarin complexone, and alizarin red S. Suisanzoshoku 51:327–335. [In Japanese with English summary.]
- McFarlane, G. A., and R. J. Beamish.
1990. An examination of age determination structures of walleye pollock (*Theragra chalcogramma*) from five stocks in the northeast Pacific Ocean. Int. North Pac. Fish. Comm. Bull. 50:37–56.
- Morita, K., and T. Matsuishi.
2001. A new model of growth back-calculation incorporating age effect based on otoliths. Can. J. Fish. Aquat. Sci. 58:1805–1811.
- Mugiya, Y.
1990. Long-term effects of hypophysectomy on the growth and calcification of otoliths and scales in the goldfish *Carassius auratus*. Zool. Sci. 7:273–279.
- Nakatani, T., and T. Maeda.
1987. Distribution and movement of walleye pollock larvae *Theragra chalcogramma* in Funka Bay and the adjacent waters, Hokkaido. Nippon Suisan Gakkaishi 53:1585–1591. [In Japanese with English summary.]
- Nishimura, A.
1993. Age determination of walleye pollock based on the otoliths (Review). In Present status and prospects of research on the biology and fisheries resources of walleye pollock and other gadid species in the waters around Hokkaido—special edition of the “Hokkaido Suketoudara Kenkyu Group” (Hokkaido Walleye Pollock Research Group) for the 25th anniversary (H. Yoshida, ed.), p.37–49. Sci. Rep. Hokkaido Fish. Exp. Stn. 42. Hokkaido Central Fisheries Experimental Station, Yoichi, Hokkaido, Japan. [In Japanese with English summary.]
- Nishimura, A., and J. Yamada.
1988. Geographical differences in early growth of walleye pollock *Theragra chalcogramma*, estimated by back-calculation of otolith daily growth increments. Mar. Biol. 97:459–465.
- Reznick, D.
1989. Slower growth results in larger otoliths: an experimental test with guppies (*Poecilia reticulata*). Can. J. Fish. Aquat. Sci. 46:108–112.
- Secor D. H., and J. M. Dean.
1992. Comparison of otolith-based back-calculation methods to determine individual growth histories of larval striped bass, *Morone saxatilis*. Can. J. Fish. Aquat. Sci. 49:1439–1454.
- Secor D. H., J. M. Dean, and E. H. Laban.
1992. Otolith removal and preparation for microstructural examination. In Otolith microstructure examination and analysis (D. K. Stevenson, and S. E. Campana, eds.), p. 19–57. Can. Spec. Publ. Fish. Aquat. Sci. 117.
- Springer, A. M.
1992. A review: walleye pollock in the North Pacific—how much difference do they really make? Fish. Oceanogr. 1:80–96.
- Traynor, J. J., W. A. Karp, T. M. Sample, M. Furusawa, T. Sasaki, K. Teshima, N. J. Williamson, and T. Yoshimura.
1990. Methodology and biological results from surveys of walleye pollock (*Theragra chalcogramma*) in the eastern Bering Sea and Aleutian Basin in 1988. Int. North Pac. Fish. Comm. Bull. 50:69–100.
- Victor, B. C.
1982. Daily otolith increments and recruitment in two coral-reef wrasses, *Thalassoma bifasciatum* and *Hali-choeres bivittatus*. Mar. Biol. 71:203–208.
- Wespestad, V. G.
1993. The status of Bering Sea pollock and effect of the “Donut Hole” fishery. Fisheries 18:18–25.
- Zeppelin, T. K., D. J. Tollit, K. A. Call, T. J. Orchard, and C. J. Gudmundson.
2004. Sizes of walleye pollock (*Theragra chalcogramma*) and Atka mackerel (*Pleurogrammus monopterygius*) consumed by the western stock of sea lions (*Eumetopias jubatus*) in Alaska from 1998 to 2000. Fish. Bull. 102: 509–521.

Appendix

The spreadsheets of the computer application Microsoft Excel (Microsoft Co., Tokyo, Japan) were used as an analysis platform, and an add-in tool solver was used for the optimization of the present OL-FL equation. The solver has been standard add-in tool in Excel since the Excel 95 version. The optimized value of the parameters and the Akaike's information criterion (AIC) in the pres-

ent equations were identical with the use of Excel 2003 and Excel 2007. The modified spreadsheet of a Microsoft Excel workbook shows how to fit the two-phase allometric smoothing function for the otolith length (OL) and fork length (FL) relationship (Appendix Table below). The most suitable equation to describe the relation between otolith length and somatic length was chosen if it accorded with the minimum AIC.

Appendix Table

The modified spreadsheet of a Microsoft Excel workbook is shown to fit the two-phase allometric smoothing function for the otolith length (OL, mm) and fork length (FL, mm) relationship in walleye pollock (*Theragra chalcogramma*) ($n=2354$). At the add-in tool of the Solver parameters dialog box in Excel, the Akaike's information criterion (AIC; cell B3) sits in the "target cell" and the parameters (cells B5 to B12) sit in the "changing cell." The optimization for the equation is a minimized AIC with adjusting parameters using solver constraints. $\hat{\sigma}_{FL_j} =$ estimated standard deviation of FL of individual j ; $f_1(OL_j) =$ calculated FL for individual j in the first function; $f_2(OL_j) =$ calculated FL for individual j in the second function; $\hat{FL}_j =$ employed calculated FL for individual j ; $L_j =$ likelihood of individual j ; $\ln L_j =$ log-likelihood of individual j ; $LL =$ a log-likelihood; $d, e, f =$ parameters for $\hat{\sigma}_{FL_j}$; $a_1, b_1, c_1 =$ parameters for $f_1(OL_j)$; and $a_2, b_2, c_2 =$ parameters for $f_2(OL_j)$; and $q_1 =$ a value of OL on the inflection point.

A	B	C	D	E	F
1	Two-phase allometric smoothing function				
2	$LL = \text{SUM}(J2:J2355)$	OL	FL	$\hat{\sigma}_{FL_j}$	$f_1(OL_j)$
3	$\text{AIC} = -2*B2+2*\text{COUNT}(B5:B12)$	1.06	37.2	$= \$B\$5*C2\wedge \$B\$6+ \$B\7	$= \$B\$8*C2\wedge \$B\$9+ \$B\10
4	Parameters	1.09	38.1	$= \$B\$5*C3\wedge \$B\$6+ \$B\7	$= \$B\$8*C3\wedge \$B\$9+ \$B\10
5	d	1.11	32.8	$= \$B\$5*C4\wedge \$B\$6+ \$B\7	$= \$B\$8*C4\wedge \$B\$9+ \$B\10
6	e	1.15	37.8	Copy down to row 2355, where $n=2354$	
7	f	1.16	36.8	2.281	38.973
8	a_1	1.17	36.9	2.288	39.169
9	b_1	1.18	35.5	2.295	39.364
10	c_1	1.23	40.8	2.329	40.332
11	q_1	1.25	39.4	2.344	40.715
12	b_2	13.73	308	24.734	175.993
13	$a_2 = B8*B9/B12*B11\wedge (B9-B12)$	13.51	351	24.173	174.222
14	$c_2 = B8*B11*B9*(1-(B9/B12))+B10$	13.76	333	24.811	176.234
		1.12	33.1	To row 2355	
1	$f_2(OL_j)$	\hat{FL}_j		I	J
2	$= \$B\$13*C2\wedge \$B\$12+ \$B\14	$= \text{IF}(C2< \$B\$11, F2, G2)$	$= \text{NORMDIST}(D2, H2, E2, \text{FALSE})$	L_j	$\ln L_j$
3	$= \$B\$13*C3\wedge \$B\$12+ \$B\14	$= \text{IF}(C3< \$B\$11, F3, G3)$	$= \text{NORMDIST}(D3, H3, E3, \text{FALSE})$		$= \text{IF}(I3<=0, -10000, \text{LN}(I3))$
4	$= \$B\$13*C4\wedge \$B\$12+ \$B\14	$= \text{IF}(C4< \$B\$11, F4, G4)$	$= \text{NORMDIST}(D4, H4, E4, \text{FALSE})$		$= \text{IF}(I4<=0, -10000, \text{LN}(I4))$
5	Copy down to row 2355, where $n=2354$				
6	42.563	38.973		0.111	-2.197
7	42.685	39.169		0.106	-2.238
8	42.807	39.364		0.042	-3.167
9	43.421	40.332		0.166	-1.793
10	43.671	40.715		0.147	-1.916
11	335.852	335.852		0.008	-4.761
12	329.204	329.204		0.011	-4.511
13	336.761	336.761		0.015	-4.141
14	To row 2355				